Journal of Machine Engineering, 2026, Vol. 26
ISSN 1895-7595 (Print) ISSN 2391-8071 (Online)

Received: *08 November 2025* /Accepted: *24 January 2026* / Published online: *16 February 2026*

EDM, ultrasonic vibration, surface roughness, material removal rate, external cylindrical surface, graphite electrode, process optimization

Thanh Van DINH[1], Quy Thu LE[2],
Loi Tat MAI[3], Pi Ngoc VU[4], Giang Ngoc TRAN[4*]

STATISTICAL MODELING AND OPTIMIZATION OF Ra AND MRR IN ULTRASONIC – ASSISTED EDM OF 90CrSi STEEL USING GRAPHITE ELECTRODES

This study investigates the modeling and single-objective optimization of surface roughness (*Ra*) and material removal rate (*MRR*) in electrical discharge machining (EDM) of external cylindrical surfaces of hardened 90CrSi tool steel. The machining process is enhanced using ultrasonic vibration assistance and graphite electrodes to improve surface integrity and productivity. Gaussian Process Regression (GPR) and Response Surface Methodology (RSM) were employed to construct predictive models for *Ra* and *MRR* based on key process parameters, including vibration amplitude (*A*), pulse-on time (*Ton*), pulse-off time (*Toff*), peak current (*IP*), and servo voltage (*SV*). The GPR model provided superior predictive performance for surface roughness, while RSM was more effective in modeling *MRR*. Optimization results showed that the minimum Ra of 1.6216 μm was achieved at A = 2.7743 μm, *Ton* = 8.0000 μs, *Toff* = 11.8294 μs, *IP* = 8.1723 A, and *SV* = 4.7936 V. Meanwhile, the maximum *MRR* of 12.1989 g/h was obtained at A = 3.5339 μm, *Ton* = 16.0000 μs, *Toff* = 8.0000 μs, *IP* = 15.0000 A, and *SV* = 4.0000 V. The findings provide valuable insights into parameter selection for improving EDM performance on external cylindrical surfaces of high-hardness steels.

1. INTRODUCTION

Electrical Discharge Machining (EDM) has become an indispensable process for fabricating complex and high-hardness components, particularly in the mold, die, and tool industries. However, conventional EDM often suffers from limitations such as low material removal rate (*MRR*), poor surface finish (*Ra*), and inefficient debris removal. To overcome these drawbacks, researchers have increasingly integrated ultrasonic vibration (UV) into EDM systems, leading to the emergence of Ultrasonic Vibration-Assisted EDM (UV-EDM) as a promising hybrid process [1–3].

[1] East Asia University of Technology (EAUT),Vietnam
[2] Research Division, National Research Institute of Mechanical Engineering (NRIME), Vietnam
[3] Faculty of Mechanical Engineering, Vinh University of Technology Education (VUTED), Vietnam
[4] Thai Nguyen University of Technology (TNUT), Vietnam
[*] E-mail: tranngocgiang@tnut.edu.vn
https://doi.org/10.36897/jme/217320

Several studies have demonstrated that UV-EDM enhances debris removal, reduces tool wear, and improves surface integrity by facilitating more stable discharges and cavitation effects in the dielectric medium [1, 4, 5]. Wang et al. [1] investigated deep-hole UV-EDM and found that longitudinal/torsional vibrations improved flushing efficiency and reduced taper. Zhang et al. [4] elucidated the role of cavitation bubbles in enhancing debris removal, whereas Dong et al. [2] developed a thermodynamic model to simulate heat distribution under vertical UV excitation. Similar insights were reported by Yin et al. [6], who introduced longitudinal-torsional vibration to improve micro-hole accuracy and machining stability.

In terms of performance enhancement, Lei et al. [6] successfully machined enclosed microgrooves using laminated electrodes under UV-EDM, achieving high precision. Li et al. [7] applied ultrasonic circular vibration (UCV) to improve surface quality in micro-hole machining, while Li et al. [8] extended this concept to analyse the integrity of machined surfaces using UCV electrodes. At the micro-scale, Ichikawa and Natsu [9] proved that ultrasonic fluid vibration facilitates machining with ultra-low discharge energy, and Xu et al. [10] emphasized the gas medium's role in material removal mechanisms when combined with UV. Despite these advances, much of the research has focused on micro-EDM, [3, 7, 8, 11], hole drilling [1, 3, 4], and specialized setups such as powder-mixed dielectric [12–14] or novel electrode configurations [6], [15]. Optimization efforts have typically targeted complex alloys like Ti-6Al-4V [11, 16, 17], cemented carbides [10, 18], or Si_3N_4 ceramics [19], but limited attention has been paid to the EDM performance of external cylindrical surfaces of hardened tool steels under ultrasonic vibration.

Moreover, although many studies have adopted Taguchi [20], ANOVA [21], FEM [22, 23], or experimental methods [24], [25], comprehensive modeling and optimization using advanced regression tools such as Gaussian Process Regression (GPR) and Response Surface Methodology (RSM) remain scarce in this context. For instance, Shabgard et al. [26, 27] and Abdullah et al. [18] used numerical modeling for UV-EDM but did not explore data-driven surrogate models. While Sundaram et al. [21] applied Taguchi-based analysis, predictive modeling of *Ra* and *MRR* using GPR and RSM on external cylindrical surfaces of 90CrSi steel has not been addressed.

In addition to ultrasonic vibration assistance, the choice of electrode material and dielectric fluid significantly influences EDM outcomes such as surface roughness and electrode wear. Anjum et al. [28] compared the performance of copper and graphite electrodes in different dielectric environments when machining AISI 304L stainless steel. Their results demonstrated that graphite electrodes, while exhibiting slightly higher tool wear, consistently provided better surface finish in hydrocarbon-based dielectrics. Similarly, Ghazi et al. [29] investigated the influence of EDM parameters on surface roughness and electrode wear rate in the machining of 7024 aluminum alloy. They emphasized the strong dependency of surface integrity on discharge energy and electrode type, underlining the importance of systematic parameter optimization for improved machining quality. These findings further justify the use of graphite electrodes in the present study and reinforce the need for comprehensive modeling of Ra and *MRR* under varying EDM conditions.

Additionally, surface topography and erosion mechanisms under UV-EDM have been studied extensively [5, 30, 31], but few investigations have quantitatively optimized both Ra and *MRR* using hybrid modeling for tool steels. Hou and Bai [32] introduced a 3D ultrasonic

vibration system to enhance debris ejection, yet did not address cylindrical geometry. Similarly, Singh et al. [22] and Choubey et al. [23] modeled ultrasonic effects on flat surfaces, but extrapolation to cylindrical geometries, which present unique spark gap dynamics, remains limited.

To address these research gaps, this study aims to develop predictive models and perform single-objective optimization of surface roughness (Ra) and material removal rate (*MRR*) in ultrasonic vibration-assisted EDM of external cylindrical surfaces of hardened 90CrSi tool steel using graphite electrodes. The process parameters considered include vibration amplitude (*A*), pulse-on time (*Ton*), pulse-off time (*Toff*), peak current (*IP*), and servo voltage (SV). GPR and RSM are employed to build accurate surrogate models for *Ra* and *MRR*, respectively. The study seeks to (i) evaluate the modeling performance of GPR vs. RSM for each response, and (ii) identify optimal parameter settings to enhance both surface finish and productivity in machining cylindrical geometries.

In contrast to prior studies that mainly employed Taguchi-based design or FEM simulations for parameter analysis, the present work introduces a data-driven surrogate modeling framework. To the best of our knowledge, this is the first study applying Gaussian Process Regression (GPR) to systematically optimize both *Ra* and *MRR* in ultrasonic vibration-assisted EDM using graphite electrodes when processing cylindrical hardened steels, a geometry that poses unique challenges compared with flat or micro-scale surfaces. Unlike multi-objective or micro-EDM investigations reported in the literature, this research deliberately focuses on single-objective optimization as a baseline step to rigorously validate the predictive accuracy of GPR against Response Surface Methodology (RSM). By establishing this foundation, the study not only demonstrates the superior modeling capability of GPR but also sets the stage for future extensions toward multi-objective optimization and intelligent process control in UV-EDM.

2. METHODOLOGY

2.1. EXPERIMENTAL SETUP AND WORKPIECE MATERIAL

An experimental investigation was carried out to evaluate the effects of five key process parameters—vibration amplitude (*A*, µm), pulse-on time (*Ton*, µs), pulse-off time (*Toff*, µs), peak current (*IP*, *A*), and servo voltage (*SV*, *V*)—on the machining performance during ultrasonic vibration-assisted electrical discharge machining (UV-EDM) of hardened tool steel. The experimental setup is illustrated in Fig. 1.

All machining operations were performed on a Sodick A30 CNC EDM machine, which was integrated with a high-power ultrasonic vibration system to improve spark stability, flushing conditions, and material removal characteristics. Ultrasonic vibrations were generated using an MPI WG-3000 ultrasonic generator (MPI Ultrasonics, Switzerland) with a rated power of 3000 W. The generated vibrations were transmitted through an RPS-5020-4Z ultrasonic transducer, operating at a frequency of 20 kHz and nominal power of 2000 W. A custom-designed titanium horn was fabricated and employed to efficiently transfer ultrasonic energy to the tool–workpiece interface, ensuring consistent vibratory motion of the electrode.

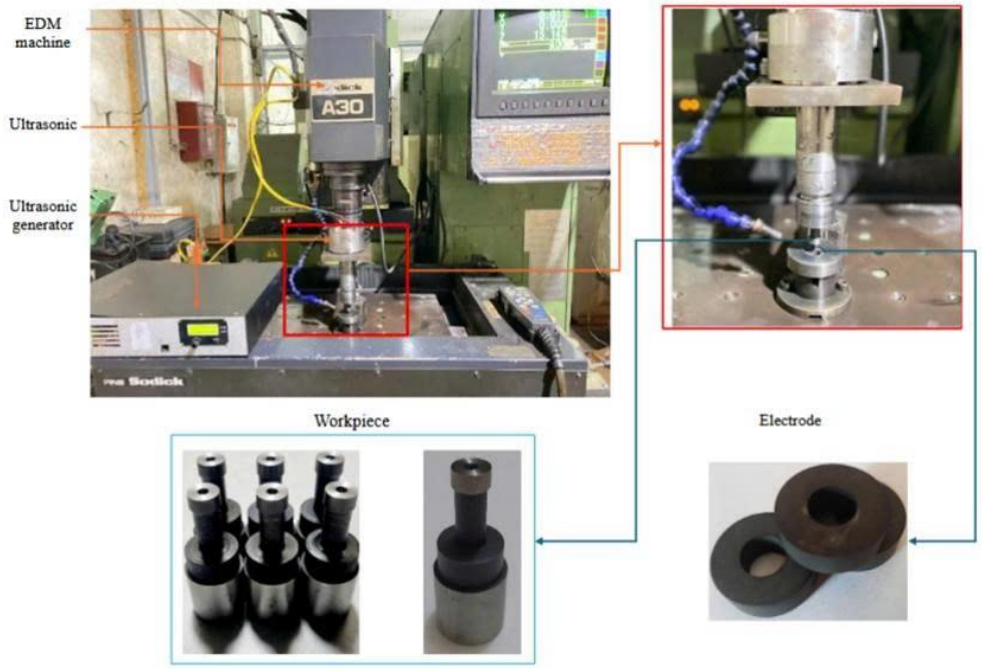

Fig. 1. Experimental setup

The tool electrode used in the experiments was made of HK0 graphite, selected for its excellent electrical conductivity, high thermal resistance, and low wear rate under discharge conditions. As the dielectric fluid, Diel MS 7000 (Total, France) was employed due to its stability and suitability for high-performance EDM applications.

The workpiece material was 90CrSi tool steel, known for its high hardness, thermal resistance, and applicability in die and mold manufacturing. The samples were cylindrical in shape to simulate real-world external surface machining conditions. The experimental dataset analysed in this work was obtained from the study by Dinh et al. [33], which investigated ultrasonic EDM of external cylindrical surfaces using graphite electrodes.

Two output responses were measured in this study: material removal rate (*MRR*) and surface roughness (Ra). The *MRR* was determined using the gravimetric method, widely accepted in EDM studies for its precision. Each workpiece was initially cleaned with ethanol, dried with warm air, and weighed using a high-precision analytical balance (accuracy: 0.1 mg). After machining, the sample was re-cleaned, re-dried, and reweighed. The *MRR* was calculated using the following equation:

$$MRR = \sum_{i=1}^{n} \frac{m_{before} - m_{after}}{t} \tag{1}$$

where m_{before} and m_{after} are the masses (in grams) of the workpiece before and after machining, and t is the machining time (in hours).

The surface roughness (Ra) was measured using a Mitutoyo SV3100 surface roughness tester. To ensure measurement accuracy and account for possible surface variability, three readings were taken at different positions along the external cylindrical surface of each machined sample. The average of these readings was reported as the final Ra value.

2.2. DESIGN OF EXPERIMENTS

To systematically investigate the influence of process parameters on material removal rate (*MRR*) and surface roughness (*Ra*), a statistical experimental design based on the Box–Behnken Design (BBD) was adopted. The experimental plan and the corresponding measured responses of *MRR* and *Ra* for each trial are presented in Table 1. This dataset served as the foundation for constructing regression models using both RSM and Gaussian Process Regression (GPR), as well as for subsequent optimization analyses.

Table. 1. Experimental plan and output

No.	*A (μm)*	*Ton (μs)*	*Toff (μs)*	*IP (A)*	*SV (V)*	*MRR (g/h)*	*Ra*
1	1.2	8	12	10	5	3.527	2.327
2	1.2	16	12	10	5	5.898	3.806
3	5.2	8	12	10	5	5.764	3.565
4	5.2	16	12	10	5	7.437	3.878
5	3.2	12	8	5	5	4.472	4.046
6	3.2	12	8	15	5	8.427	5.548
7	3.2	12	16	5	5	3.844	3.879
8	3.2	12	16	15	5	7.941	4.627
9	3.2	8	12	10	4	5.738	2.201
10	3.2	8	12	10	6	6.019	2.767
11	3.2	16	12	10	4	9.391	4.835
12	3.2	16	12	10	6	9.182	3.039
13	1.2	12	8	10	5	4.351	3.945
14	1.2	12	16	10	5	3.531	3.070
15	5.2	12	8	10	5	6.380	3.846
16	5.2	12	16	10	5	4.933	3.553
17	3.2	12	12	5	4	3.659	4.201
18	3.2	12	12	5	6	3.810	3.927
19	3.2	12	12	15	4	8.024	5.981
20	3.2	12	12	15	6	8.017	6.189
21	3.2	8	8	10	5	6.081	1.915
22	3.2	8	16	10	5	6.323	1.838
23	3.2	16	8	10	5	9.737	5.153
24	3.2	16	16	10	5	8.178	4.662
25	1.2	12	12	5	5	2.582	4.405
26	1.2	12	12	15	5	5.488	4.815
27	5.2	12	12	5	5	3.436	4.080
28	5.2	12	12	15	5	7.274	4.574
29	3.2	12	8	10	4	9.035	3.174
30	3.2	12	8	10	6	6.832	3.128
31	3.2	12	16	10	4	7.255	3.464
32	3.2	12	16	10	6	7.068	4.003
33	1.2	12	12	10	4	4.510	4.059
34	1.2	12	12	10	6	5.475	3.205
35	5.2	12	12	10	4	4.879	3.091
36	5.2	12	12	10	6	5.066	3.792
37	3.2	8	12	5	5	2.703	2.093
38	3.2	8	12	15	5	5.674	3.461
39	3.2	16	12	5	5	6.862	1.818
40	3.2	16	12	15	5	10.239	10.627
41	3.2	12	12	10	5	6.426	4.098
42	3.2	12	12	10	5	7.386	3.976
43	3.2	12	12	10	5	7.481	3.913
44	3.2	12	12	10	5	7.634	4.020
45	3.2	12	12	10	5	6.282	3.859
46	3.2	12	12	10	5	7.717	3.969

BBD is an efficient response surface methodology (RSM) approach suitable for modeling nonlinear relationships and minimizing the number of required experimental runs without compromising the quality of statistical analysis.

The five input parameters considered in this study were vibration amplitude (A), pulse-on time (*Ton*), pulse-off time (*Toff*), peak current (*IP*), and servo voltage (*SV*). Specifically, vibration amplitude (*A*) represents the level of ultrasonic vibration applied to the electrode, measured in micrometers (μm). Pulse-on time (*Ton*) is the duration of each electrical discharge pulse, while pulse-off time (*Toff*) denotes the interval between successive discharges; both are expressed in microseconds (μs). Peak current (*IP*), measured in amperes (*A*), refers to the maximum current delivered during each discharge. Finally, servo voltage (*SV*), measured in volts (*V*), regulates the inter-electrode gap to maintain stable spark conditions throughout the machining process.

Each factor was varied at three levels (low, center, high), and the parameter ranges were determined based on preliminary trials and machine constraints. Also, the parameter ranges and BBD experimental matrix were adopted from the work of Dinh et al. [33]. The BBD matrix included 46 experimental runs, ensuring a balanced distribution of design points across the multidimensional design space while avoiding extreme combinations that may risk tool or workpiece damage.

3. RESULTS AND DISCUSSION

3.1. REGRESSION MODELING OF Ra AND *MRR* USING RSM

To quantify the relationship between the five input parameters and the machining responses, quadratic regression models for surface roughness (Ra) and material removal rate (*MRR*) were developed using Response Surface Methodology (RSM). These models were constructed based on the experimental data obtained from the Box–Behnken Design (BBD) and implemented using MATLAB scripting combined with statistical computation. All regression coefficients were estimated via least-squares fitting, and model quality was evaluated through R^2 and adjusted R^2 metrics.

RSM Model for Surface Roughness (Ra):

The fitted second-order polynomial equation for Ra is expressed as:

$$\begin{aligned} Ra = {} & -1.8271 - 0.3543A + 0.9024Ton + 0.2958Toff - 1.6659IP + 2.0133SV - 0.0365A.\\ & Ton + 0.0182A, Toff + 0.0021A, IP + 0.1943A, SV - 0.0065Ton, Toff + 0.0930Ton,\\ & IP - 0.1476Ton, SV - 0.0094Toff, IP + 0.0366Toff, SV + 0.0241IP, SV - 0.0619A^2\\ & - 0.0260Ton^2 - 0.0163Toff^2 + 0.0376IP^2 - 0.1604SV^2 \end{aligned} \quad (2)$$

This model yielded an R^2 of 0.7780 and an adjusted R^2 of 0.6003, indicating only a moderate fit to the experimental data. Among the input variables, peak current (*IP*) was statistically significant ($p = 0.0168$), while the interaction *Ton* × *IP* was highly significant ($p = 0.0003$), reflecting the strong influence of discharge energy on surface finish. Nevertheless, the low adjusted R^2 suggests that the model lacks the capacity to fully capture

the nonlinear nature of *Ra* in ultrasonic-assisted EDM. The performance of the model is illustrated in Fig. 2, which shows a noticeable spread in predicted vs. actual *Ra* values.

RSM Model for Material Removal Rate (*MRR*):

The RSM model for *MRR* is expressed as:

$$\begin{aligned} MRR = {} & -6.9146 + 4.2114A + 0.3313Ton - 0.3702Toff + 1.0368IP - 0.6301SV - 0.0218A \\ & Ton - 0.0196A, Toff + 0.0233A, IP - 0.0974A, SV - 0.0281Ton, Toff + 0.0051Ton, \\ & IP - 0.0306Ton, SV + 0.0018Toff, IP + 0.1260Toff, SV - 0.0079IP, SV - 0.4928A^2 \\ & + 0.0283Ton^2 + 0.0011Toff^2 - 0.0391IP^2 - 0.0188SV^2 \end{aligned} \quad (3)$$

This model achieved a higher level of reliability, with $R^2 = 0.9238$ and adjusted $R^2 = 0.8628$, indicating strong predictive capability. The most influential factors were vibration amplitude (A) with $p = 0.0032$ and IP with borderline significance ($p = 0.0579$). The squared terms of A^2 and IP^2 were also significant, indicating nonlinear relationships with *MRR*.

As shown in Fig. 3, the model predictions align closely with experimental results, confirming the suitability of RSM for modeling *MRR* in this context.

While the RSM model for *MRR* demonstrated high fidelity with an adjusted R^2 of 0.8628 and acceptable statistical significance for key terms, it is important to note that the model still assumes a fixed quadratic structure, which may limit its generalization in regions outside the experimental domain. Therefore, to further enhance modeling robustness and predictive *accuracy for both Ra and MRR – especially given the moderate fit of the Ra model (adjusted* $R^2 = 0.6003$) – a more flexible and nonparametric approach, namely Gaussian Process Regression (GPR), was adopted. The development and evaluation of GPR-based surrogate models are detailed in the following section.

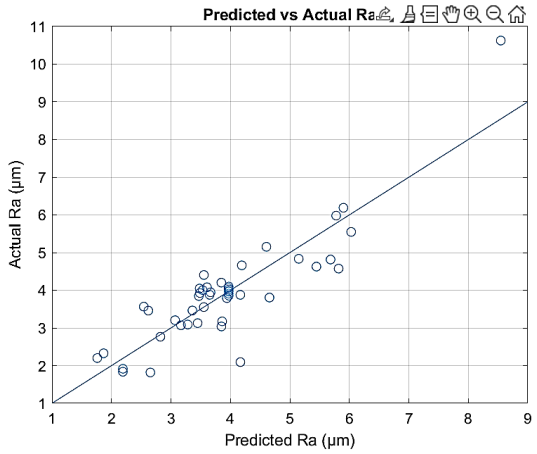

Fig. 2. Predicted vs. Actual Surface Roughness (*Ra*) Using RSM Model results

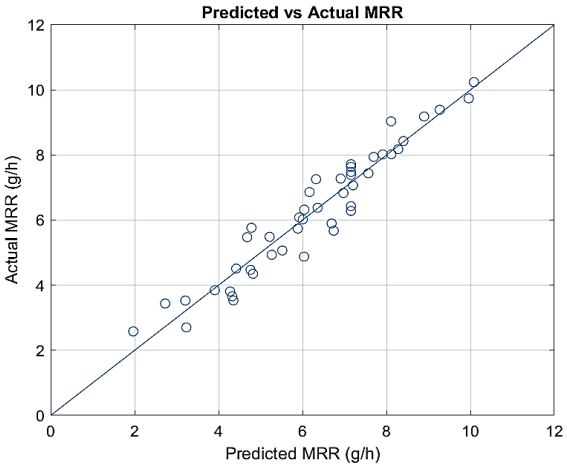

Fig. 3. Predicted vs. Actual *MRR* using RSM Model

3.2. SURROGATE MODELING USING GPR

To improve predictive accuracy beyond what was achievable with second-order polynomial regression, Gaussian Process Regression (GPR) was employed as a surrogate modeling approach for both surface roughness (*Ra*) and material removal rate (*MRR*). Unlike

RSM, which imposes a fixed quadratic structure, GPR provides a data-driven, nonparametric method capable of capturing complex interactions and nonlinearities inherent in ultrasonic vibration-assisted EDM processes.

3.2.1. GPR MODELING FOR SURFACE ROUGHNESS(RA)

Given the relatively low adjusted R^2 (0.6003) of the RSM model for *Ra*, GPR was applied with various kernel and basis function combinations to explore improvements in accuracy. The combinations evaluated include squared exponential, rational quadratic, Matern 3/2, and Matern 5/2 kernels, each paired with constant, linear, or pure quadratic basis functions.

As shown, multiple combinations yielded high R^2 values; however, the Matern 3/2 kernel with constant basis was selected for its combination of high accuracy, model simplicity, and numerical stability, achieving $R^2 = 0.9996$ (Table 2).

The predictive performance of this selected model is illustrated in Fig. 4, which displays the close alignment between predicted and actual *Ra* values.

Table 2. Summarizes the results for all kernel–basis configurations evaluated for Ra

Kernel	Basis Function	R^2	Adjusted R^2
Squared Exponential	Constant	0.9996	0.9996
Squared Exponential	Linear	0.9907	0.9895
Squared Exponential	Pure Quadratic	0.5928	0.5419
Rational Quadratic	Constant	0.9858	0.9840
Rational Quadratic	Linear	0.9996	0.9996
Rational Quadratic	Pure Quadratic	0.9996	0.9996
Matern 3/2	Constant	0.9996	0.9996
Matern 3/2	Linear	0.9780	0.9753
Matern 3/2	Pure Quadratic	0.9996	0.9996
Matern 5/2	Constant	0.9491	0.9427
Matern 5/2	Linear	0.9768	0.9739
Matern 5/2	Pure Quadratic	0.5928	0.5419

3.2.2. GPR MODELING FOR MATERIAL RATE(MMR)

Although the RSM model for *MRR* exhibited strong performance (adjusted $R^2 = 0.8628$), GPR was applied to further enhance prediction accuracy and provide a unified surrogate modeling framework for both responses. Similar to the *Ra* modeling process, various kernel–basis combinations were tested.

Several combinations offered nearly identical performance; however, the Matern 5/2 kernel with linear basis was selected due to its balance of high accuracy and lower computational complexity, yielding $R^2 = 0.9881$ and adjusted $R^2 = 0.9866$. The predicted vs. actual plot for this GPR-*MRR* model is shown in Fig. 5, highlighting the model's excellent predictive capability. Table 3 presents the results of all combinations evaluated for *MRR*.

Table 3. GPR Model Comparison for Material Removal Rate (*MRR*)

Kernel	Basis Function	R^2	Adjusted R^2
Squared Exponential	Constant	0.9375	0.9297
Squared Exponential	Linear	0.9881	0.9866
Squared Exponential	Pure Quadratic	0.9881	0.9866
Rational Quadratic	Constant	0.9429	0.9357
Rational Quadratic	Linear	0.9881	0.9866
Rational Quadratic	Pure Quadratic	0.9881	0.9866
Matern 3/2	Constant	0.9881	0.9866
Matern 3/2	Linear	0.9881	0.9866
Matern 3/2	Pure Quadratic	0.9881	0.9866
Matern 5/2	Linear	0.9881	0.9866
Matern 5/2	Constant	0.9873	0.9858
Matern 5/2	Pure Quadratic	0.9881	0.9866

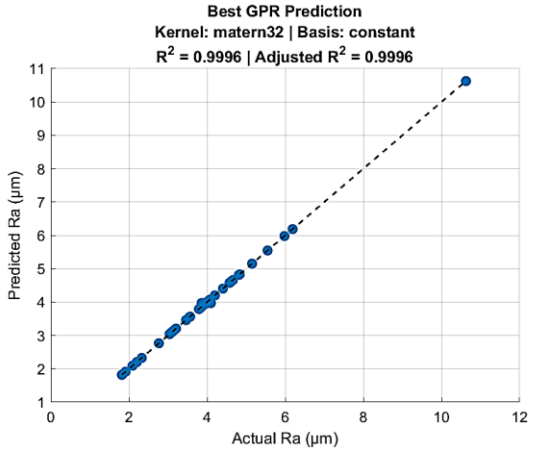

Fig. 4. Predicted vs. Actual Ra Values Using the Best GPR Model (Kernel: Matern 3/2, Basis:

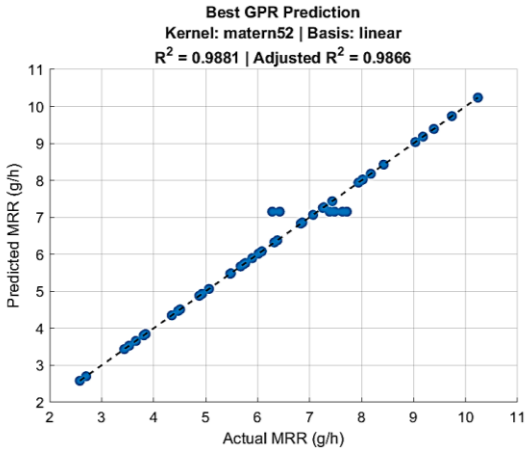

Fig. 5. Predicted vs. Actual *MRR* Using the Best GPR Model (Kernel: Matern 5/2, Basis: Linear)

3.2.3. SUMMARY OF MODEL PERFORMANCE COMPARISON

To objectively compare the modelling performance of RSM and GPR for both *Ra* and MRR, the key performance indicators –R^2, adjusted R^2, root mean square error (RMSE), and mean absolute error (MAE) – were computed and summarized in Table 4.

Table 4. Comparison of Predictive Accuracy Between RSM and GPR Models

Response	Model	R^2	Adjusted R^2	RMSE	MAE
Ra	RSM	0.7780	0.6003	0.2947	0.2582
Ra	GPR	0.9996	0.9996	0.0213	0.0164
MRR	RSM	0.9238	0.8628	0.3584	0.2941
MRR	GPR	0.9881	0.9866	0.1487	0.1175

In summary, the GPR models significantly outperformed their RSM counterparts, particularly for Ra, where the RMSE decreased by more than 90% ($\frac{0.2947-0.0213}{0.2947} \cdot 100 = 92.77\%$), and the R^2 improved from 0.7780 to 0.9996. The GPR model for *MRR* also yielded superior performance over RSM despite RSM's already strong fit. Based on these results, the GPR models were selected for the subsequent optimization process described in Section 3.3.

3.3. OPTIMIZATION AND ANALYSIS OF OPTIMAL CONDITIONS

Based on the superior predictive performance of the Gaussian Process Regression (GPR) models for both material removal rate (*MRR*) and surface roughness (*Ra*), single-objective optimization was conducted to identify the best possible machining parameter settings for each response. The optimization process aimed to:

- Maximize *MRR* using the GPR model with the Matern 5/2 kernel and linear basis,
- Minimize Ra using the GPR model with the Matern 3/2 kernel and constant basis.

The optimization was performed in MATLAB using a combination of global and local search techniques. The optimal parameter combinations obtained from the surrogate models are summarized below.

3.3.1. OPTIMIZATION FOR MAXIMUM MRR

Using the GPR surrogate for *MRR*, the following input settings were identified as optimal: Vibration amplitude (*A*): 5.2000 µm, Pulse-on time (*Ton*): 16.0000 µs, Pulse-off time (*Toff*): 8.0000 µs, Peak current (*IP*): 15.0000 A, and Servo voltage (*SV*): 4.0000 V. At these conditions, the predicted maximum *MRR* was 10.6379 g/h.

This optimal setting corresponds to high electrical energy (Ton, IP) and maximum ultrasonic amplitude, which collectively enhance plasma channel formation and debris evacuation, resulting in higher erosion rates. Notably, this condition aligns with trends observed in the GPR model: *MRR* increases with increasing *A* and *IP*, while excessively high *Toff* or *SV* contributes little to material removal.

3.3.2. OPTIMIZATION FOR MINIMUM Ra

The GPR model for Ra suggested the following optimal parameter combination for achieving the best surface finish: Vibration amplitude (*A*): 2.9380 µm, Pulse-on time (*Ton*): 8.0000 µs, Pulse-off time (*Toff*): 12.0830 µs, Peak current (IP): 5.7544 *A*, and Servo voltage (*SV*): 4.7723 V. Under these settings, the predicted minimum surface roughness was 2.0407 µm. This optimal configuration reflects a moderate vibration amplitude, short pulse-on time, and low-to-moderate current, which collectively contribute to milder discharges and more uniform crater formation, resulting in smoother surface texture. Higher servo voltage (*SV*) and longer *Toff* intervals help stabilize the gap and allow sufficient time for debris clearance.

3.3.3. COMPARATIVE OBSERVATIONS

A comparison of the optimal conditions for *Ra* and *MRR* reveals an expected performance trade-off:

- Achieving high *MRR* requires aggressive discharge settings and strong vibration, which tend to deteriorate surface quality.

- In contrast, minimizing Ra necessitates gentler discharge energy and more balanced flushing intervals.

This confirms the classic conflict in EDM between productivity and surface integrity, reinforcing the value of applying multi-objective optimization in future studies. A summary of the optimal solutions is presented in Table 7.

Table 7. Optimal Conditions and Predicted Responses Based on GPR Models

Objective	*A* (µm)	*Ton* (µs)	*Toff* (µs)	*IP* (A)	*SV* (V)	Predicted Response
Maximize *MRR*	5.2000	16.0000	8.0000	15.0000	4.0000	10.6379 g/h
Minimize Ra	2.9380	8.0000	12.0830	5.7544	4.7723	2.407

3.4. VALIDATION OF OPTIMAL CONDITIONS

To verify the reliability of the developed GPR surrogate models for both *MRR* and *Ra*, validation experiments were conducted using the respective optimal parameter settings predicted in Section 3.3. The actual machining responses obtained from these trials were compared with the predicted values to assess the accuracy of the models.

3.4.1. VALIDATION OF THE GPR MODEL FOR *MRR*

The GPR model for *MRR* suggested the following optimal machining condition for maximizing material removal rate:

Vibration amplitude (*A*) = 5.2000 µm, Pulse-on time (*Ton*) = 16.00 µs, Pulse-off time (*Toff*) = 8.00 µs, Peak current (IP) = 15.00 A, and Servo voltage (*SV*) = 4.00 V, which yielded a predicted *MRR* of 10.6379 g/h.

To validate this prediction, an EDM experiment was performed using machine-adjusted practical values as follows:

A = 1.52 µm, *Ton* = 16 µs, *Toff* = 8 µs, *IP* = 15 A, and *SV* = 4 V.

The *MRR* was computed based on the weight loss of the workpiece before and after machining, using a high-precision electronic balance. The resulting measured *MRR* was 10.352 g/h, yielding a relative error of only 2.69% compared to the GPR-predicted value.

This small deviation confirms the high predictive accuracy and practical applicability of the GPR model for *MRR* under ultrasonic vibration-assisted EDM conditions.

3.4.2. VALIDATION OF THE GPR MODEL FOR Ra

The GPR model for Ra identified the following optimal combination for achieving minimal surface roughness:

Vibration amplitude (*A*) = 2.9380 µm, Pulse-on time (*Ton*) = 8.0000 µs, Pulse-off time (*Toff*) = 12.0830 µs, Peak current (*IP*) = 5.7544 A, and Servo voltage (*SV*) = 4.7723 V, resulting in a predicted *Ra* of 2.0407 µm.

A validation test was performed using approximated real machine input values: A = 2.94 µm, Ton = 8 µs, $Toff$ = 12.1 µs, IP = 6 A, and SV = 5.8 V.

The measured surface roughness was Ra = 1.962 µm, leading to a relative error of 3.86% from the model prediction.

This low deviation further validates the predictive strength of the GPR model for Ra and confirms its ability to guide parameter selection for improved surface quality.

These validation results support the use of GPR as a robust surrogate modeling framework for ultrasonic-assisted EDM, demonstrating both high predictive fidelity and practical feasibility in real machining environments.

3.5. DISCUSSION AND INTERPRETATION

The optimization results obtained in Section 3.3 clearly demonstrate the opposing trends and inherent trade-offs between material removal rate (*MRR*) and surface roughness (*Ra*) in ultrasonic vibration-assisted EDM of 90CrSi steel. This duality is a well-known challenge in non-traditional machining, where enhanced productivity often comes at the expense of surface integrity.

Trade-off Between Surface Quality and Material Removal

The optimal condition for maximizing MRR involves a high discharge energy regime - characterized by long pulse-on time (*Ton*), high peak current (*IP*), and maximum ultrasonic amplitude (A = 5.2 µm). While these parameters promote rapid material erosion through more intense plasma channels and enhanced cavitation-assisted flushing, they also increase the thermal load and result in deeper, more chaotic craters on the workpiece surface.

Conversely, the configuration that minimizes Ra requires moderate vibration ($A \approx 2.9$ µm), lower *IP*, and extended *Toff*. These settings reduce the discharge energy per pulse and allow better stabilization of the inter-electrode gap, thus favouring smoother surface formation. However, this comes with a significant reduction in machining efficiency, as evident from the lower predicted *MRR* at the *Ra*-optimal condition.

This inverse relationship is visualized in the response surfaces generated by the GPR models (not shown here), where regions of high *MRR* correspond to elevated *Ra* values, and vice versa. It highlights the necessity of compromise or multi-objective decision-making when both surface finish and machining speed are of concern.

Role of Ultrasonic Vibration in Balancing Performance

Ultrasonic vibration contributes positively to both objectives, but in different magnitudes and forms:

- For *MRR*, higher amplitude amplifies cavitation effects, debris displacement, and secondary discharge events, resulting in accelerated material removal.
- For Ra, moderate amplitude helps in maintaining discharge stability and reducing localized thermal accumulation, which minimizes surface defects.

Thus, amplitude control is a critical lever in process tuning. The identified optimal amplitudes (5.2 µm for *MRR* and 2.9 µm for *Ra*) provide quantitative targets for real-time process adjustment, particularly in CNC-EDM systems integrated with intelligent controllers.

Implications for Practical Application

From a practical standpoint, the findings provide clear guidance for process engineers:

- When surface finish is critical (e.g., die cavity finishing, sealing surfaces), the Ra-optimal condition should be prioritized.

- When removal rate dominates (e.g., roughing or high-throughput applications), the *MRR*-optimal condition is more suitable.

- In cases where both objectives are important, these two solutions can serve as boundary anchors for multi-objective optimization using evolutionary algorithms (e.g., NSGA-II, MOEA/D).

Although GPR outperformed RSM in predictive accuracy, their practical roles differ. RSM yields simple quadratic equations that are easy to interpret and thus useful for rapid analysis and preliminary process guidance. GPR, while computationally more demanding and less interpretable, provides much higher accuracy for predicting optimal *Ra* and *MRR*. In this study, RSM was used for quick insights, whereas GPR ensured reliable optimization, highlighting their complementary value in both practical and advanced applications. Moreover, the successful application of GPR as a surrogate modeling tool demonstrates its value for developing digital twins of EDM systems—capable of real-time prediction and optimization in smart manufacturing contexts.

4. CONCLUSION

This study investigated the modeling and single-objective optimization of surface roughness (Ra) and material removal rate (*MRR*) in the ultrasonic vibration-assisted electrical discharge machining (UV-EDM) of external cylindrical 90CrSi steel using graphite electrodes. Two surrogate modeling techniques—Response Surface Methodology (RSM) and Gaussian Process Regression (GPR)—were developed and evaluated to predict the machining responses as functions of five process parameters: vibration amplitude (*A*), pulse-on time (*Ton*), pulse-off time (*Toff*), peak current (*IP*), and servo voltage (*SV*).

The RSM model for *MRR* demonstrated good predictive performance (adjusted R^2 = 0.8628), while the RSM model for *Ra* showed only moderate fit (adjusted R^2 = 0.6003), indicating limitations in capturing nonlinear behavior. In contrast, the GPR models significantly improved prediction accuracy for both responses. The best GPR configurations Matern 5/2 kernel with linear basis for *MRR*, and Matern 3/2 kernel with constant basis for *Ra*—achieved adjusted R^2 values of 0.9866 and 0.9996, respectively. The RMSE values for GPR models were reduced by 58% for *MRR* and over 92% for *Ra* when compared to RSM.

Using the GPR models, optimal parameter settings were determined for each objective. The predicted maximum *MRR* was 10.6379 g/h, and the minimum *Ra* was 2.0407 μm. Validation experiments performed under machine-adjusted practical conditions yielded errors of only 2.69% (*MRR*) and 3.86% (*Ra*), thereby confirming the reliability and practical applicability of the GPR-based surrogate modeling and optimization approach.

REFERENCES

[1] WANG P., et al., 2025, *Debris Motion and Taper Suppression in EDM Deep Hole Machining Assisted by Longitudinal/Torsional Ultrasonic Vibration*, Journal of Manufacturing Processes, 133, 798–810.

[2] DONG Y., LIU J., LI G., WANG Y., 2022, *Thermodynamic Simulation Modeling Analysis and Experimental*

Research of Vertical Ultrasonic Vibration Assisted EDM, The International Journal of Advanced Manufacturing Technology, 119/7, 5303–5314.

[3] YIN Z. et al., 2023, *A Novel EDM Method Using Longitudinal-Torsional Ultrasonic Vibration (LTV) Electrodes to Improve Machining Performance for Micro-Holes*, Journal of Manufacturing Processes, 102, 231–243.

[4] ZHANG P. et al., 2024, *Investigating Mechanisms of Debris Removal in Ultrasonic Vibration-Assisted EDM Drilling*, International Journal of Mechanical Sciences, 279, 109486.

[5] WANG Y., FAN L., SHI J., DONG Y., FU Z., 2023, *Effect of Cavitation on Surface Formation Mechanism of Ultrasonic Vibration-Assisted EDM*, The International Journal of Advanced Manufacturing Technology, 124/10, 3645–3656.

[6] LEI J., SHEN H., WU H., PAN W., WU X., ZHAO C., 2024, *Ultrasonic Vibration-Assisted Electrical Discharge Machining of Enclosed Microgrooves with Laminated Electrodes*, Journal of Materials Research and Technology, 30, 9521–9530.

[7] LI Z., TANG J., BAI J., 2020, *A Novel Micro-EDM Method to Improve Microhole Machining Performances Using Ultrasonic Circular Vibration (UCV) Electrode*, International Journal of Mechanical Sciences, 175, 105574.

[8] LI Z., TANG J., LI Y., BAI J., 2022, *Investigation on Surface Integrity in Novel Micro-EDM with Two-Dimensional Ultrasonic Circular Vibration (UCV) Electrode*, J. Manuf. Process. 76, 828–840.

[9] ICHIKAWA T., NATSU W., 2013, *Realization of Micro-EDM Under Ultra-Small Discharge Energy by Applying Ultrasonic Vibration to Machining Fluid*, Procedia CIRP, 6, 326–331.

[10] XU M., ZHANG J., LI Y., ZHANG Q., REN S., 2009, *Material Removal Mechanisms of Cemented Carbides Machined by Ultrasonic Vibration Assisted EDM in Gas Medium*, Journal of materials processing technology, 209/4, 1742–1746.

[11] XU J., XIA S., YU P., LI M., 2024, *Multi-Objective Parameter Optimization of Ultrasonic Vibration–Assisted Micro-EDM Of Ti-6Al-4V Alloys*, Journal of Vibration and Control, 30/7–8, 1818–1828.

[12] BUI V.D., et al., 2024, *Ultrasonic Vibration Assisted Silver Integration by Powder Mixed EDM for Antibacterial Surfaces*, Procedia CIRP, 123, 410–415.

[13] HAN J., GAO X., ZHOU Y., LI Z., GAO M., ZHANG Q., 2024, *Machining Characteristics in Ultrasonic Vibration-Assisted Powder-Mixed Electrical Discharge Machining of Tin Ceramics*, Ceramics International, 50/8, 13478–13489.

[14] LI M., ZHANG T., FU L., DING L., XIE L., 2025, *Research on the Strengthening Layer of TC4 Alloy Strengthened by Ultrasonic Vibration-Assisted Powder-Mixed Near-Dry Multi-Dielectrics EDM*, Journal of Mechanical Science and Technology, 1–8.

[15] CHENXUE W., SASAKI T., HIRAO A., 2022, *Observation of Bubble Behavior in EDM with Ultrasonic Vibration*, Procedia CIRP, 113, 267–272.

[16] ZHANG P. et al., 2023, *Experimental Research and Multi-Objective Optimization of Ultrasonic Vibration–Assisted EDM for Ti6Al4V Micro-Holes*, The International Journal of Advanced Manufacturing Technology, 127/7, 3413–3425.

[17] SINGH P., YADAVA V., NARAYAN A., 2018, *Parametric Study of Ultrasonic-Assisted Hole Sinking Micro-EDM of Titanium Alloy*, The International Journal of Advanced Manufacturing Technology, 94, 2551–2562.

[18] ABDULLAH A., SHABGARD M.R., 2008, *Effect of Ultrasonic Vibration of Tool on Electrical Discharge Machining of Cemented Tungsten Carbide (WC-Co)*, The International Journal of Advanced Manufacturing Technology, 38, 1137–1147.

[19] PRANEETPONGRUNG C., FUKUZAWA Y., NAGASAWA S., YAMASHITA K., 2010, *Effects of the EDM Combined Ultrasonic Vibration on the Machining Properties of Si3N4*, Materials Transactions, 51/11, 2113–2120.

[20] PRIHANDANA G.S., MAHARDIKA M., HAMDI M., WONG Y.S., MITSUI K., 2009, *Effect of Micro-Powder Suspension and Ultrasonic Vibration of Dielectric Fluid in Micro-EDM Processes–Taguchi Approach*, International Journal of Machine Tools and Manufacture, 49/12–13, 1035–1041.

[21] SUNDARAM M.M., PAVALARAJAN G.B., RAJURKAR K.P., 2008, *A Study on Process Parameters of Ultrasonic Assisted Micro EDM Based on Taguchi Method*, Journal of Materials Engineering and Performance, 17, 210–215.

[22] SINGH J., WALIA R., SATSANGI P., SINGH V., 2011, FEM *Modeling of Ultrasonic Vibration Assisted Work-Piece in EDM Process*, International Journal of Mechanic Systems Engineering, 1/1, 8–16.

[23] CHOUBEY M., MAITY K., SHARMA A., 2020, *Finite Element Modeling of Material Removal Rate in Micro-EDM Process With and Without Ultrasonic Vibration*, Grey Systems: Theory and Application, 10/3, 311–319.

[24] KREMER D., LHIAUBET C., MOISAN A., 1991, *A Study of the Effect of Synchronizing Ultrasonic Vibrations with Pulses in EDM*, CIRP annals, 40/1, 211–214.

[25] SINGH G., SATSANGI P., PRAJAPATI D., 2020, *Effect of Rotating Magnetic Field and Ultrasonic Vibration on Micro-EDM Process*, Arabian Journal for Science and Engineering, 45/2, 1059–1070.

[26] SHABGARD M.R., GHOLIPOOR A., MOHAMMADPOURFARD M., 2018, *Numerical and experimental study of the effects of ultrasonic vibrations of tool on machining characteristics of EDM process*, The International Journal of Advanced Manufacturing Technology, 96, 2657–2669.

[27] SHERVANI-TABAR M.T., MAGHSOUDI K., SHABGARD M.R., 2013, *Effects of Simultaneous Ultrasonic Vibration of the Tool and the Workpiece in Ultrasonic Assisted EDM*, International Journal for Computational Methods in Engineering Science and Mechanics, 14/1, 1–9.

[28] ANJUM S., SHAH M., ANJUM N., MEHMOOD S., ANWAR W., 2017, *Machining and Surface Characteristicso of AISI 304L after Electric Discharge Machining for Copper and Graphite Electrodes in Different Dielectric Liquids, Engineering*, Technology & Applied Science Research, 7/4, 1765–1770.

[29] GHAZI S.K., ABDULLAH M.A., ABDULRIDHA H.H., 2025, *Investigating the Impact of EDM Parameters on Surface Roughness and Electrode Wear Rate in 7024 Aluminum Alloy*, Engineering, Technology & Applied Science Research, 15/1, 19401–19407.

[30] HOU S., BAI J., LIU H., ZHOU Z., LU Z., 2023, *Study on Material Erosion Mechanism of Ultrasonic Vibration-Assisted Micro-EDM Based on Heat-Flow Coupling Analysis*, The International Journal of Advanced Manufacturing Technology, 125/1 465–478.

[31] DONG Y., et al., 2024, *Study on Mechanism and Surface Topography of Ultrasonic Powder Mixing–Assisted EDM*, The International Journal of Advanced Manufacturing Technology, 135/1, 337–350.

[32] HOU S., BAI J., 2023, *A Novel Ultrasonic Vibration-Assisted Micro-EDM Method to Improve Debris Removal Performance Using Relative Three-Dimensional Ultrasonic Vibration (RTDUV)*, The International Journal of Advanced Manufacturing Technology, 127/11–12, 5711–5727.

[33] DINH V.-T., LE T.-Q., VU D.-B., VU N.-P., MAI T.-L., 2025, *Ultrasonic EDM for External Cylindrical Surface Machining with Graphite Electrodes: Horn Design and Hybrid NSGA-II–AHP Optimization of MRR and R*, Machines, 13/8, 675.